Grain-size gap and downstream fining revealed in less chemically altered Brahmaputra Sandbars

Abhishek Dixit[1] · Subashisa Dutta[1] · Chandan Mahanta[1]

Abstract

Purpose Limited studies exist on the downstream variation of grain size in sand-bed rivers, particularly in natural sediment regimes. The impact of local grain-size variability, lateral tributaries, and bedrock confined zones on the downstream trend remains underexplored.

Methods We examined 54 sediment samples from the sandbars of the Brahmaputra main trunk, analyzing grain size and bulk mineralogy, along with selected samples for clay mineralogy. End-member modeling was applied to the grain-size data, and existing depth profile data were used to propose a transport mechanism.

Results and discussion The Brahmaputra sandbar sediments are less chemically altered as indicated by low kaolinite (ca. 10%) and high illite (ca. 70%) content. The median grain sizes of sandbar samples vary from 17 μm to 356 μm. This variability is attributed to the low-width bedrock-confined zones, characterized by increased grain size, local flow conditions, and selective transportation deposition of sediments within specific size classes. Additionally, we observed a notable scarcity of samples having a dominant mode in the intermediate range of approximately 63–172 μm. This grain-size gap is explained by the proposed transport mechanism, with sediments within the gap selectively transported during peak discharge periods, coarsening the riverbed and depleting sediments within the 63–172 μm range over repeated annual floods. Sediments below 63 μm are consistently present in the water column and can be deposited in low-flow zones within floodplains.

Conclusion Results corroborate previous studies indicating limited chemical weathering in the Brahmaputra basin. The implications of our results extend to downstream fining, sand-mud transition, and formation of grain-size gaps in sand-bed rivers.

Keywords Grain-size analysis · End-member modeling · Brahmaputra · Sand-mud transition · Grain-size gap · Downstream fining

1 Introduction

Understanding the composition and processes of sediment in river floodplains is essential for unraveling sediment provenance and dynamics in fluvial basins (e.g., Johnsson 1993; Weltje and von Eynatten 2004). These floodplain environments, influenced by lithology, physical and chemical processes, act as reservoirs of mixed sediments from various tributaries. Hydrodynamic processes, driven by changes in flow conditions, selectively entrain and sort sediments,

resulting in variations in grain size and composition. Chemical weathering within floodplains also plays a significant role, impacting sediment composition and revealing distinct weathering signatures (Lupker et al. 2012; Bouchez et al. 2012). In sand-bed rivers, downstream sediment fining occurs, leading to a progressive reduction in grain size (Frings 2008), with implications for interpreting weathering signals and sediment composition (von Eynatten et al. 2012; von Eynatten et al. 2016).

The significance of sediment grain size extends beyond river hydraulics and morphology; it is also a controlling parameter for the mineralogical and chemical composition of sediments (von Eynatten et al. 2012; von Eynatten et al. 2016). For example, Dixit et al. (2023) demonstrated that grain size can explain ca. 50% of the chemical variability in suspended load, with floodplain sediments playing a crucial role in determining the sediment transported in suspension.

✉ Abhishek Dixit
abhishek.dixit@iitg.ac.in

1 Department of Civil Engineering, Indian Institute
of Technology Guwahati, Guwahati, Assam 781039, India

While significant progress has been made in understanding the downstream variation of grain size in gravel-bed rivers (see review by Dingle et al. 2021), studies focusing specifically on sand-bed rivers remain scarce (Frings 2008).

Existing studies on sand-bed rivers are predominantly conducted on small rivers or anthropologically regulated rivers (Ta et al. 2011; Luo et al. 2012; Musselman and Tarbox 2013; He et al. 2022; He et al. 2023), with fewer reports from rivers still maintaining a relatively less regulated sediment regime. One example is the study by Singh et al. (2007), which reported a downstream fining rate of 2% per 100 km in the Ganga River. However, the downstream fining trend, often described by an exponential function, can be disrupted by lateral tributaries joining the main channel, resulting in a local maximum of grain size within the main channel (e.g., Singh et al. 2007; Ta et al. 2011; Luo et al. 2012; Pan et al. 2015). A similar effect on grain size can be caused by bedrock confined zones within the river, which are characterized by a decrease in channel width over a short longitudinal length. Perhaps due to the relative rarity of this morphological feature, it has remained under-reported (Wang et al. 2009).

Moreover, the downstream fining trend is typically derived by averaging out the local variability in samples collected from nearby locations or by selecting samples from the same deposition environment. However, at local scales, the median grain size can exhibit significant variation, ranging from approximately 20 μm to 250 μm (Singh et al. 2007). This local variability, which has not been extensively discussed, can significantly impact the downstream trend (Rice and Church 2010) and is worth exploring as it may reveal distinct river processes.

In the case of the Brahmaputra River, while sediment samples have been collected from its floodplains to determine the proportions of sediment sources (Singh and France-Lanord 2002; Garzanti et al. 2004; Lupker et al. 2017; Gemignani et al. 2018), a detailed investigation of the downstream variation in sediment composition at a finer resolution is lacking, despite the river's dynamic braiding patterns within the floodplains (Nandi et al. 2022).

In this study, we conduct an analysis of sediment grain size and bulk mineralogy of 54 samples from 31 locations in a reach of ca. 500 km, as well as clay mineral analysis for selected samples to understand the downstream variation of grain size and mineral composition in the Brahmaputra floodplains. Firstly, we examine the presence or absence of the grain-size gap, a phenomenon frequently observed in gravel-bed rivers, within the context of a sand-bed river. Then, we aim to elucidate the trend of downstream fining in a sand-bed river and its correlation with variations in the river's width. Simultaneously, we investigate a potential interplay between this fining trend and chemical weathering patterns.

2 Study area

The Brahmaputra River traverses diverse landscapes, connecting various terrains. Originating from the Tibetan Plateau and making a notable turn at the Eastern Syntaxis, the river meanders through floodplains, receiving contributions from numerous tributaries, before finally reaching the Bengal Delta (Fig. 1a and b). The channel bottom slope at Pasighat is about 0.62 m km^{-1} which reduces to 0.11 m km^{-1} near Guwahati and finally 0.079 m km^{-1} in Bengal Delta (Sarma 2005).

The Brahmaputra River is known for its high sediment load, with an estimated annual sediment delivery ranging from 500 to 1000 Mt (Goswami 1985; Islam et al. 1999; Galy and France-Lanord 2001; Milliman and Farnsworth 2011). Sediment sources are heterogeneously distributed across the basin, with the Eastern Syntaxis accounting for more than 50% of the sediment input in floodplains (Singh and France-Lanord 2002; Garzanti et al. 2004; Lupker et al. 2017; Gemignani et al. 2018), despite the presence of northern and southern tributaries. Sediments in the Brahmaputra basin are primarily derived from physical weathering processes (Garzanti et al. 2004; Khan et al. 2019), with mass wasting events such as landslides being significant contributors (Wasson et al. 2022).

The floodplains of the Brahmaputra exhibit intricate braiding patterns characterized by the presence of sand bars, low-flow channels, chutes, cut-offs, and vegetated landforms (Nandi et al. 2022). Within the floodplains, the Brahmaputra River exhibits three distinct narrow and low-braiding zones known as nodes, where the river is constrained by bedrock. These nodal points, namely Guwahati, Tezpur, and Goalpara (Fig. 1), remain morphologically stable despite changing flow conditions and river shifting. The river width at nodal points is ca. 1 km, whereas, it can reach up to 18 km with the presence of multiple active channels at different locations.

3 Sampling and methodology

3.1 Sampling

In January 2021, during the non-monsoon season when the sandbars were exposed, we conducted our sampling campaign along the Brahmaputra trunk, specifically targeting the bar tops and freshly exposed channel bars within the Majuli to Dhubri reach (Fig. 1b). It is important to note that the part of the exposed sandbars we sampled is submerged annually with the onset of the first monsoon flood, as documented by Dixit et al. (2023). These sandbars represent dynamic landforms subject to annual erosion and deposition. To minimize potential bias, we avoided sampling vegetated sandbars. In cases where vegetation was present nearby, we positioned our sampling locations
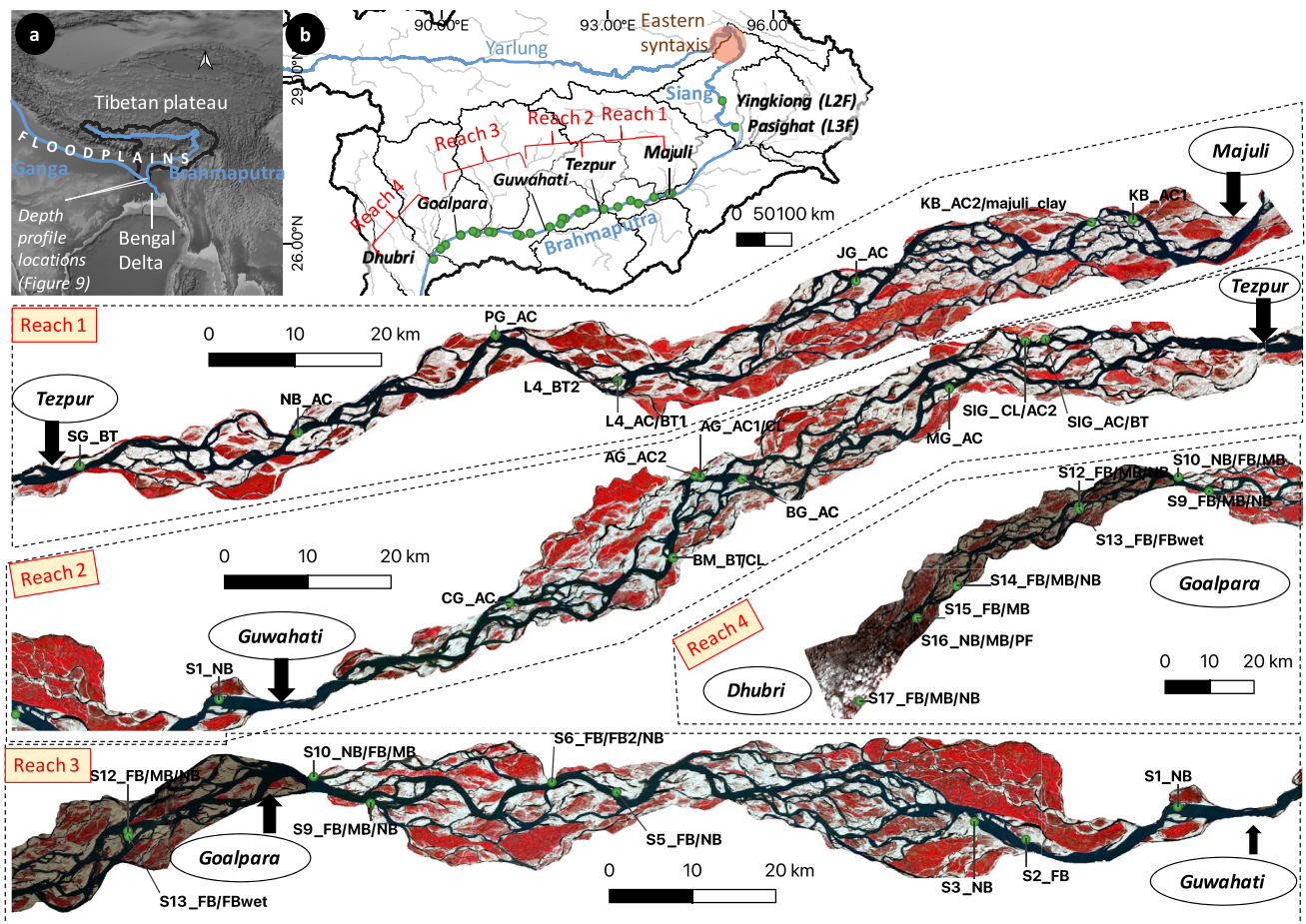
Fig. 1 a Location of the Brahmaputra basin covering the part of Tibetan plateau, floodplains, and Bengal Delta. **b** Path of the Brahmaputra River in Tibetan plateau (Yarlung), Himalaya (Siang), and Brahmaputra in floodplains. Locations of bed samples collected are shown by green dots. Four reaches in Majuli-Tezpur-Guwahati-Goalpara-Dhubri are highlighted. Morphological patterns of these reaches are individually shown in each reach satellite image (Reach 1, Reach 2, Reach 3, and Reach 4) along with the location and codes of samples collected from sandbars. Satellite images for reaches are taken from Sentinel 2 for January 2021 and presented in standard false color composite. Red represents vegetation, dark blue is water and cyan are exposed sandbars

at a distance to focus on landforms consistently influenced by fluvial processes and actively part of the river channel. Additionally, two samples from the Siang tributary were collected in November 2019. We collected sediment samples from the uppermost layer of the bar, carefully removing the top 10–20 cm of sediment from the surface. In cases where visually distinct sediment deposits were observed, we sampled them separately to capture their unique characteristics. At each location, we collected between 1 and 3 sediment samples, resulting in a total of 54 samples collected from 31 locations.

3.2 Grain-size analysis and end-member modeling

3.2.1 Grain-size analysis

Grain-size distribution of sediments was determined using the Malvern Particle Analyzer (Mastersizer 2000).

To achieve proper dispersion, samples were treated with Sodium Hexametaphosphate and subsequently sonicated in an ultrasonic bath. The Hydro 2000 MU (A) accessory served as the dispersion unit in the Malvern Particle Analyzer. Initially, a 500 ml beaker was prepared to contain the sample for dispersion and subsequent delivery to the optical unit. The beaker was filled with deionized water, and background values were accurately measured. The sample, dispersed and sonicated, was carefully introduced into the beaker drop by drop. Obscuration was maintained at approximately 15%. A pump speed of 2500 rpm was employed for optimal dispersion. To prevent cross-contamination, thorough flushing of the accessory and beaker was conducted between measurements. The volume percentages of grain-size classes were then measured within the range of 0.01–10,000 μm and compiled into datasets.

The grain-size distribution can be effectively interpreted using the C-M plot, a valuable tool for understanding sediment transport and deposition dynamics (Passega 1964; Passega and Byramjee 1969; Ludwikowska-Kędzia 2013). Samples aligned along the C=M line are classified as graded suspensions. Sediment deposits in this zone are formed by the suspended sediments near the river bed maintained by the bottom turbulence to keep the coarsest fraction in suspension. The division between uniform and graded suspension occurs at M=100 μm, where M < 100 μm deposits are formed by sediments suspended in a uniform suspension. Sediment deposits in this zone suggest that these deposits likely formed during the receding flood stage, characterized by diminished sediment carrying capacity, which led to the deposition of sediments. The rolling zone appears at higher C values compared to graded suspension, while over-bank pool suspension deposits are characterized by lower C and M values than graded and uniform suspension. More details and exact boundaries of the C-M plot zones can be obtained from the Passega (1964), Passega and Byramjee (1969) and Ludwikowska-Kędzia (2013).

3.2.2 End-member modeling

To identify geologically meaningful end-members and estimate their relative abundance, an end-member modeling algorithm (EMA) was applied. EMA, initially introduced by Weltje (1997) for compositional data, has been adapted for grain-size data analysis by Prins and Weltje (1999).

In EMA algorithms, it is assumed that the observed data is a linear combination of the end-members. Mathematically, the unmixing problem can be expressed as $X = AS + E$, where X represents the observed data (with each sample as a row), A is the abundance matrix of the constituent end-members represented by S (with each end-member as a row), and E accounts for sampling and measurement errors. This equation is subject to non-negativity and sum-to-one constraints. These constraints ensure that abundances cannot be negative and must represent relative proportions that sum to a constant.

After the work of Prins and Weltje (1999), various EMA algorithms have been developed specifically for grain-size data analysis (see review by Van Hateren et al. 2018). One notable algorithm is the Hierarchical Alternating Least Squares Nonnegative Matrix Factorization (HALS-NMF) introduced by Paterson and Heslop (2015). The NMF algorithm seeks to find two nonnegative matrices, A and S, that approximately satisfy the equation $X \approx AS$. By enforcing the nonnegativity constraints on A and S, NMF proves to be a robust approach for solving grain-size distribution unmixing problems. The detailed algorithmic procedure is provided in the supplementary information of Paterson and Heslop (2015).

3.3 Bulk mineralogy

X-ray diffraction (XRD) analysis was conducted to determine the major mineral phases present in the samples. Prior to analysis, the samples were gently ground using a mortar and pestle. XRD scans were performed using the Rigaku TTRAX III instrument, operating at 5 kW with Cu-Kα radiation ($\lambda = 1.5406$ Å). The scanning range spanned from 3 to 70° for the 2θ angle, with a scan step of 0.02° and a scan speed of 20° per minute. The relative proportions of quartz, feldspar, and sheet silicates were determined based on the maximum intensity peaks within the 2θ ranges of 26–27° 27.5−28.5° and 8–10° respectively.

3.4 Clay mineralogy

The clay mineralogy analysis involved XRD of oriented clay mounts obtained from the <2 μm size fraction. To prepare the samples, dried sediments were initially treated with 30% H_2O_2 to eliminate organic matter, followed by multiple rinses with demineralized water to remove chemical residues. The <2 μm size fraction was separated based on Stokes' law, and a concentrated paste of the desired fraction was spread onto a glass slide using the filter peel method.

The prepared samples were treated with ethylene glycol solvation for 48 h at 60°C and then scanned within the range of 3° to 30°. The major clay minerals, namely smectite, illite, kaolinite, and chlorite, were identified by calculating the integrated peak areas at 7 Å (smectite), 10 Å (illite), and 17 Å (kaolinite + chlorite), after applying empirical factors of 1, 4, and 2, respectively, as described by Biscay (1965). The relative proportions of kaolinite and chlorite were determined using the peak-intensity ratio of 3.57 Å to 3.54 Å. We adopted a methodology similar to Khan et al. (2019), who examined clay mineralogy in the bed sediments of the Bengal Delta, to ensure better comparability with their dataset.

4 Results

4.1 Grain-size distributions

The statistics of the grain-size distributions of all samples are tabulated in Table 1. The sediment samples collected from the sandbars of the Brahmaputra primarily fall within the coarse silt to fine sand size range. The grain-size distributions of the samples display modes centered either around ca. 20 μm or ca. 200 μm (Fig. 2). Notably, the grain-size distribution of the sediment samples reveals a limited number of samples within the 63–172 μm range. Sediments in this size range mostly belong to either the coarse tail of fine sediments or fine tail of coarse sediments. We emphasize that this range does not exhibit a distinct boundary, but

Table 1 Geometric grain-size statistics (in μm) of the samples collected from the Brahmaputra basin

Sl. no	Sample code	Latitude	Longitude	Distance (km)	Mean	Median	Coarsest first percentile	Dominant mode
1	S17_FB	25.72	89.85	473.7	48	54	264	69
2	S17_MB	25.72	89.85	473.7	22	24	110	35
3	S17_NB	25.72	89.85	473.7	57	63	302	79
4	S16_NB	25.90	89.98	449.3	32	33	249	46
5	S16_MB	25.90	89.98	449.3	185	195	473	209
6	S16_PF	25.90	89.98	449.3	29	28	387	30
7	S15_MB	25.90	89.98	449.3	16	16	105	20
8	S15_FB	25.90	89.98	449.3	73	76	666	91
9	S14_NB	25.97	90.07	437.4	27	24	434	26
10	S14_MB	25.97	90.07	437.4	19	18	411	20
11	S14_FB	25.97	90.07	437.4	352	344	705	363
12	S13_FB	26.15	90.35	403.9	61	56	447	46
13	S13_FBwet	26.15	90.35	403.9	37	38	353	46
14	S12_FB	26.15	90.35	403.9	159	207	650	316
15	S12_MB	26.15	90.35	403.9	282	290	655	316
16	S12_NB	26.15	90.35	403.9	166	196	577	240
17	S10_NB	26.22	90.57	380.0	19	20	98	23
18	S10_MB	26.22	90.57	380.0	124	179	468	240
19	S10_FB	26.22	90.57	380.0	102	151	447	209
20	S9_NB	26.19	90.64	372.1	38	40	358	52
21	S9_MB	26.19	90.64	372.1	30	30	249	35
22	S9_FB	26.19	90.64	372.1	223	208	460	209
23	S6_NB	26.21	90.85	350.1	34	37	360	52
24	S6_FB2	26.21	90.85	350.1	51	52	260	60
25	S6_FB	26.21	90.85	350.1	205	223	577	275
26	S5_NB	26.20	90.93	342.2	216	230	569	240
27	S5_FB	26.20	90.93	342.2	191	210	470	240
28	S3_NB	26.16	91.36	299.2	412	418	822	479
29	S2_FB	26.14	91.42	299.2	187	229	625	316
30	S1_NB	26.18	91.61	273.0	174	279	708	363
31	CG_AC	26.30	91.95	237.8	281	281	625	316
32	BM_CL	26.35	92.15	216.1	17	18	138	23
33	BM_BT	26.35	92.15	216.1	101	105	401	120
34	AG_AC2	26.45	92.18	205.6	215	216	525	240
35	AG_CL	26.45	92.18	205.6	19	18	321	20
36	AG_AC1	26.45	92.18	205.6	234	241	603	275
37	BG_AC	26.45	92.23	199.8	54	57	458	69
38	MG_AC	26.56	92.48	172.3	358	378	1039	417
39	SIG_AC2	26.61	92.57	161.2	189	216	621	275
40	SIG_CL	26.61	92.57	161.2	23	23	248	30
41	SIG_AC	26.62	92.60	158.8	227	212	448	240
42	SIG_BT	26.62	92.60	158.8	118	120	635	138
43	SG_BT	26.62	92.93	125.5	236	247	569	275
44	NB_AC	26.66	93.18	99.9	234	252	599	275
45	PG_AC	26.77	93.41	73.9	103	101	253	105
46	L4_BT2	26.72	93.56	58.6	177	168	695	182
47	L4_BT1	26.72	93.56	58.6	185	187	823	417
48	L4_AC	26.72	93.56	58.6	196	204	690	275
49	JG_AC	26.84	93.83	28.1	208	217	614	275

Table 1 (continued)

Sl. no	Sample code	Latitude	Longitude	Distance (km)	Mean	Median	Coarsest first percentile	Dominant mode
50	majuli_clay	26.91	94.11	0.0	18	16	337	17
51	KB_AC1	26.91	94.16	0.0	89	88	370	91
52	KB_AC2	26.91	94.11	0.0	59	60	451	209
53	L3F	28.10	95.30	Pasighat	211	955	1905	209
54	L2F	28.57	95.07	Yingkiong	1245	177	549	1259

rather demonstrates a general paucity of sediments in this intermediate size range. Henceforth, we will refer the range of this gap in the grain-size distribution as the 63–172 μm size range. Overall, the samples display poor sorting and a fine-skewed distribution, with only a few coarse sediments (fine sand) showing well-sorted characteristics. The grain-size distribution curve of the coarsest sediments corresponds to the Yingkiong region in the Siang valley (Figs. 1 and 3a). Notably, the sediments at the outlet of Siang River (Pasighat, Fig. 1b) attain a similar grain-size distribution as floodplain sediments.

Further insights are provided by the C-M plot illustrated in Fig. 4. The C-M plot, based on the coarsest first percentile (C) and median grain size (M), aids in distinguishing different depositional environments (Passega 1964; Passega and Byramjee 1969; Ludwikowska-Kędzia 2013). The majority of our sandbar sediments are primarily located within the uniform suspension and graded suspension (saltation) zones. Our samples did not exhibit any deposits within the rolling zone, which is characterized by higher C values than observed. Additionally, a few samples exhibited characteristics of over-bank pool suspension deposits, indicating the presence of favorable conditions for water

stagnation on the surface. This was observed in the field for samples BM_BT and BM_CL, as illustrated in Fig. 4. These samples revealed a layered deposit, with fine-grained, BM_CL overlaying the coarse-grained, BM_BT, formed within a depression on a sandbar that facilitated over-bank pool suspension deposition.

4.2 End-member modeling

The goodness-of-fit statistics of HALS-NMF algorithm indicate that the four end-member model is well-optimized, with a linear coefficient of determination greater than 0.9 for all samples and a median angular deviation of less than 15° (Fig. 5a and b). The end-member model consists of a grain-size mean of approximately 18, 90, 215, and 395 μm for the four end-members, EM 1, EM 2, EM 3, and EM 4, respectively (Fig. 5c). The grain-size distribution of the finest end-member, EM 1, closely resembles the grain-size distribution reported previously for suspended sediments in the Brahmaputra River (Garzanti et al. 2011; Dixit et al. 2023). The grain-size distribution statistics of top water surface suspended sediments in the Bengal Delta, with a mean of 18 μm, skewness of 0.3, and kurtosis of 3 is similar to EM 1.
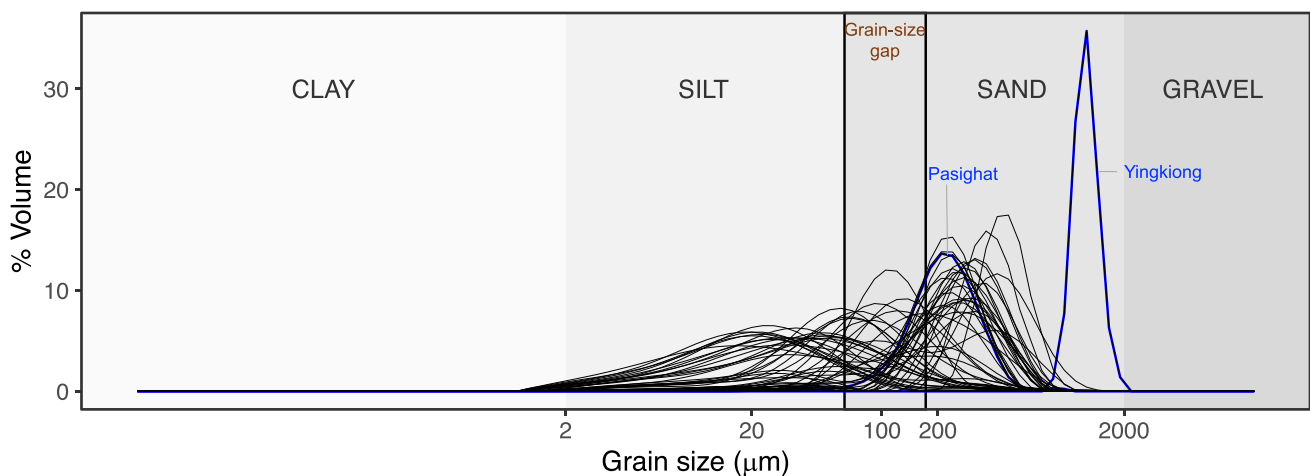

Fig. 2 Grain-size distribution of 54 samples along the Brahmaputra main trunk and Siang River. Two vertical lines delineate the size range of 63–172 μm, roughly indicating a relatively less sediments within this particular range

Fig. 3 Field photographs captured during the low-flow period (September-2019 and January-2021) showing variability of sediment deposits. **a** shows bed sediments along with boulders at Yingkiong in Siang valley, **b** shows the fine-grained sediments deposited by the slowly receding flood over the slope of sandbar, **c** shows the coarse-grained bar-top, **d** and **e** show the examples of slowly emerging sandbars in floodplains, **f** sandbar depression
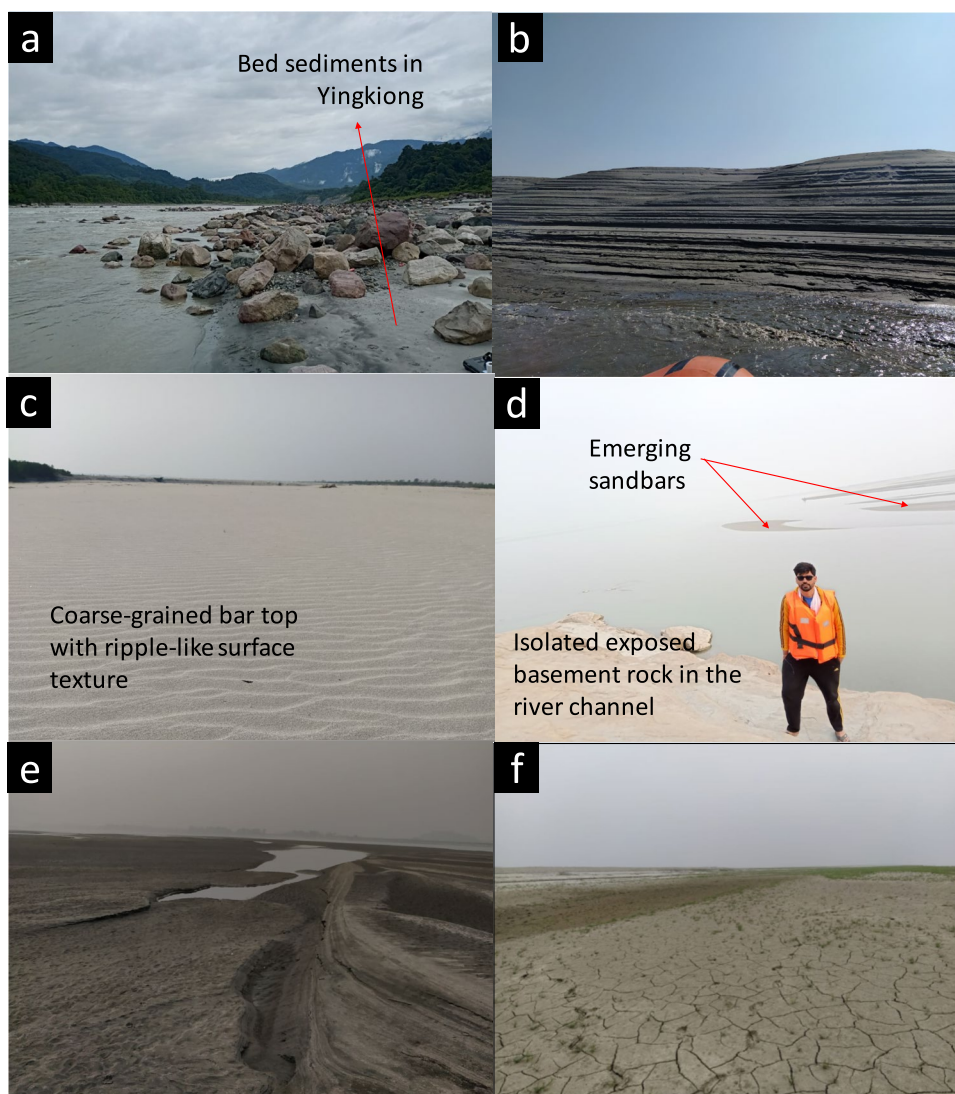

Figure 6 shows the relative abundance of end-members across three deposition environments in the C-M plot. Graded suspension deposits are predominantly composed of coarse-grained end-members (EM 3 and EM 4), while uniform suspension deposits are dominated by fine-grained end-members (EM 1 and EM 2). Over-bank pool suspension deposits primarily consist of EM 1. The subordinate abundance of EM 2 is observed in all three deposition zones (Table 2). On average, graded suspension deposits contain 16.8% EM 2 and 52.9% EM 3, while uniform suspension deposits contain 34.2% EM 2 and 61.5% EM 1. Furthermore, 74% of samples in uniform suspension and 90% in graded suspension exhibit less than 50% abundance of EM 2. The lower abundance of EM 2 (90.02 μm) aligns with the grain-size gap (63–172 μm) as depicted in Fig. 2.

The sediment samples collected near Guwahati and Tezpur demonstrate a pronounced occurrence of the coarse end-members, EM 3 and EM 4, while the downstream regions are primarily characterized by the presence of the fine end-members, EM 1 and EM 2. Notably, certain intermediate samples (e.g., BM_CL, AG_CL, SIG_CL) exhibit a dominance of EM 1, potentially influenced by local low-flow conditions, as illustrated in the inset of Fig 4.

4.3 Qualitative bulk mineralogy

The qualitative bulk mineralogy analysis using XRD consistently reveals a dominant peak corresponding to quartz in the analyzed samples. This is followed by the presence of feldspar and sheet silicates, as depicted in Fig. 7. Minor peaks of amphibole, smectite, and chlorite were also detected. This mineral assemblage aligns well with the previously reported mineral composition of the Brahmaputra River (Garzanti et al. 2010; Garzanti et al. 2011; Dixit et al. 2023). Since quantitative mineral proportions were not determined, ratios of peak intensities

Fig. 4 C-M plot comparing the coarsest first percentile (C) and median grain size (M), illustrating three distinct deposition zones according to Passega (1964), Passega and Byramjee (1969) and Ludwikowska-Kędzia (2013). The inset shows a field observed case of layer deposition of two samples BM_BT and BM_CL, aligning with the deposition zones of suspension and over-bank pool suspension, respectively

5 Discussion

5.1 Local variability of grain-size distribution
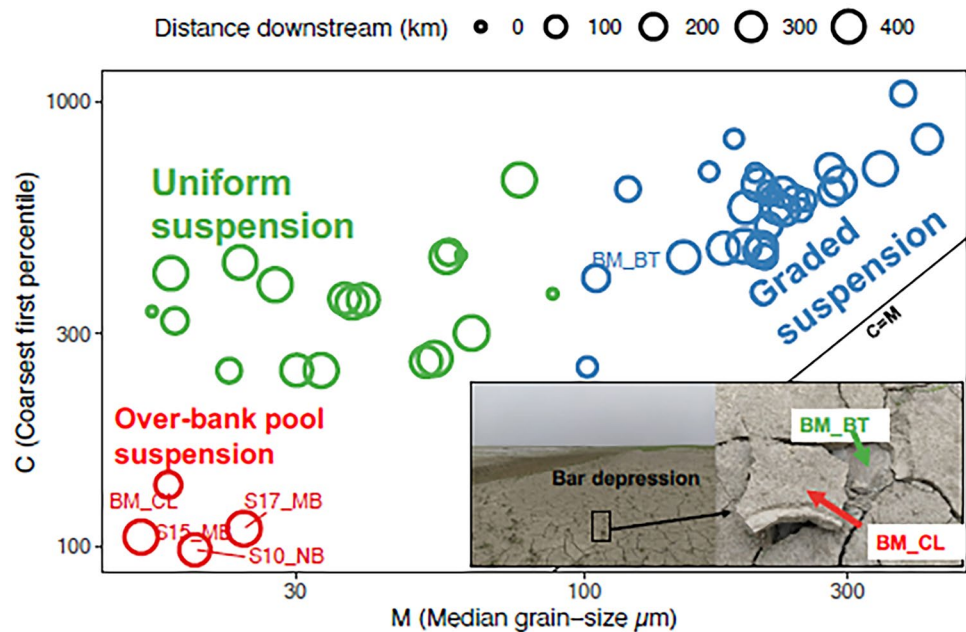
for different mineral phases were utilized as a proxy for their relative proportions. Notably, the intensity ratios of quartz to sheet silicates exhibit a positive correlation with the median grain size, as shown in the inset of Fig. 7. This correlation aligns with the grain-size effect on mineralogy, where quartz tends to be enriched in the coarser fraction and sheet silicates in the finer fraction (Lupker et al. 2011; Garzanti et al. 2011).

4.4 Clay mineralogy

Clay mineralogy analysis was conducted on a specific subset of samples, namely majuli_clay, SIG_CL, AG_CL, BM_CL, S6_NB, S16_PF, and S17_MB, which exhibited a higher proportion (> 50%) of fine-grained material belonging to end-member EM 1. The dominant clay minerals identified were illite and chlorite, accounting for an average proportion of approximately 65% and 20%, respectively (Fig. 8). The presence of kaolinite varied from 5% to 25% without a distinct pattern along the main trunk. The prevalence of illite and chlorite, with a lesser amount of kaolinite, suggests a predominance of physical weathering processes and limited chemical weathering within the floodplains. The relatively lower abundance of smectite can be attributed to the lesser occurrence of mafic rocks in the basin (Khan et al. 2019; Garzanti 2019). These observations align with expectations, considering that smectite is typically associated with the weathering of mafic minerals (Khan et al. 2019). Furthermore, these findings are consistent with the clay mineralogy reported in the bed sediments of the Bengal Delta Khan et al. (2019), who reported similar clay mineral proportions (77% illite, 10% kaolinite, 11% chlorite, and 2% smectite).

The grain-size distribution of sandbars can exhibit significant variability, which appears to be influenced by the local flow conditions during sediment deposition. For instance, samples collected from the same sandbars, such as AG_AC1 and AG_CL, BM_BT and BM_CL, and S14_MB and S14_NB, display different abundances of grain-size end-members (Fig. 6). Even in cases where the end-members are similar between samples from different locations, such as BM_CL and AG_CL, they can correspond to distinct deposition environments. For instance, BM_CL represents over-bank pool suspension deposition, whereas AG_CL represents suspension deposits (Fig. 4).

5.2 Grain-size gap and transport mechanism

Figure 2 reveals a relatively small number of samples having a dominant mode in the grain-size distribution curve within the size range of approximately 63–172 μm (EM 2). This is particularly evident in the inset of Fig. 7, where the median values of most samples (83%) lie outside of this size range. This indicates that sandbar deposits are predominantly composed of either too-fine sediment (ca. 20 μm) or too-coarse sediment (ca. 200 μm), with intermediate size range (63–172 μm) sediments being distributed in the coarse or fine tails of the grain-size distribution curves. Such grain-size distribution patterns can be attributed to the selective transport and supply limit as well as flow conditions in which the sediments are deposited. To make our
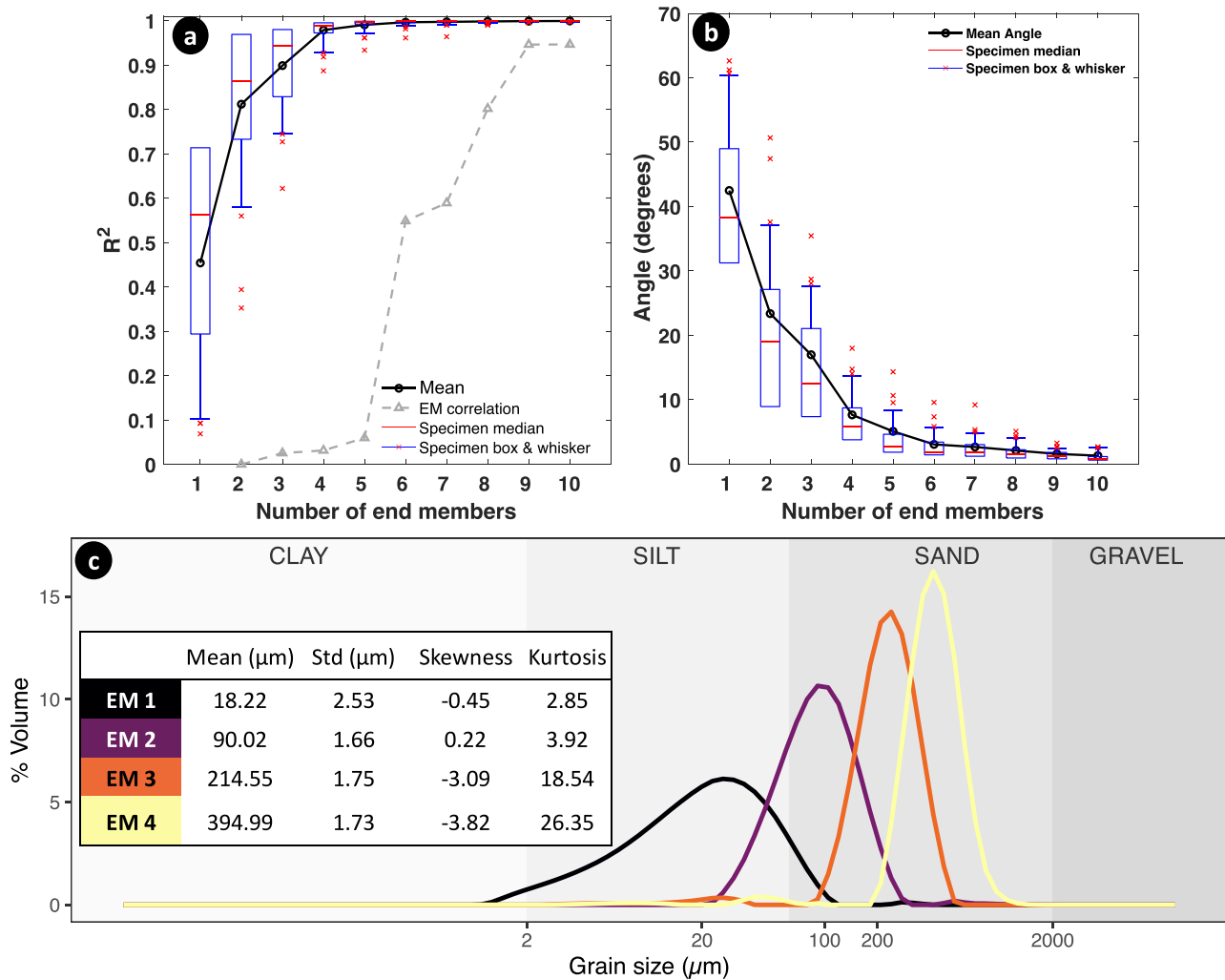
Fig. 5 Goodness-of-fit statistics of the end-member model. **a** and **b** show the coefficient of determination and angular deviation, respectively, between the original grain-size distribution and calculated grain-size distribution by different end-member models. The red bars are the median values, the blue boxes are the interquartile range, and the blue whiskers mark out the one-sided 95th percentiles to represent the lowest quality fits. The red crosses represent outlying specimens (i.e., specimens that lie outside of the 95% coverage interval). EM correlation shows the correlation among the grain-size distribution of end-members. Four end-member model was selected for end-member abundance calculation. **c** Grain-size distribution of end-members and their geometric method of moments statistics, i.e., mean, sorting (Std), skewness, and kurtosis

arguments, we draw upon previously collected sediment data from depth profiles of the Ganga (Lupker et al. 2011) and Brahmaputra (Garzanti et al. 2011) Rivers in the Bengal Delta. Ganga and Brahmaputra Rivers share geological, climatic, and morphological similarities, making them suitable for a valid comparison. Additionally, we align our hypothesis with the findings of a relevant study conducted in the Ganga basin by Singh et al. (2007).

Depth profile data (Fig. 9) shows that the sediments in the 63–172 μm size range are suspended near the bed which is characterized by the graded suspension. However, this is observed only during peak and rising discharge periods. The low flow and receding discharge consistently carry the sediments in the size-range of uniform suspension (ca. 20 μm). Too-coarse sediments exist in the bed sediments and too-fine sediments are transported in the upper water column. The absence of sediments within the 63–172 μm during low flow and receding discharge periods suggests that these sediments are transported downstream during peak flow, resulting in a slight coarsening of the riverbed. In the absence of fresh sediment supply, repeated annual floods would progressively coarsen the upstream riverbed, and eventually would be depleted in this size range. Consequently, a higher proportion of sediments within the 63–172 μm size range should be visible downstream, either in floodplains or in deltaic and oceanic bed sediment. However, our data from the floodplains
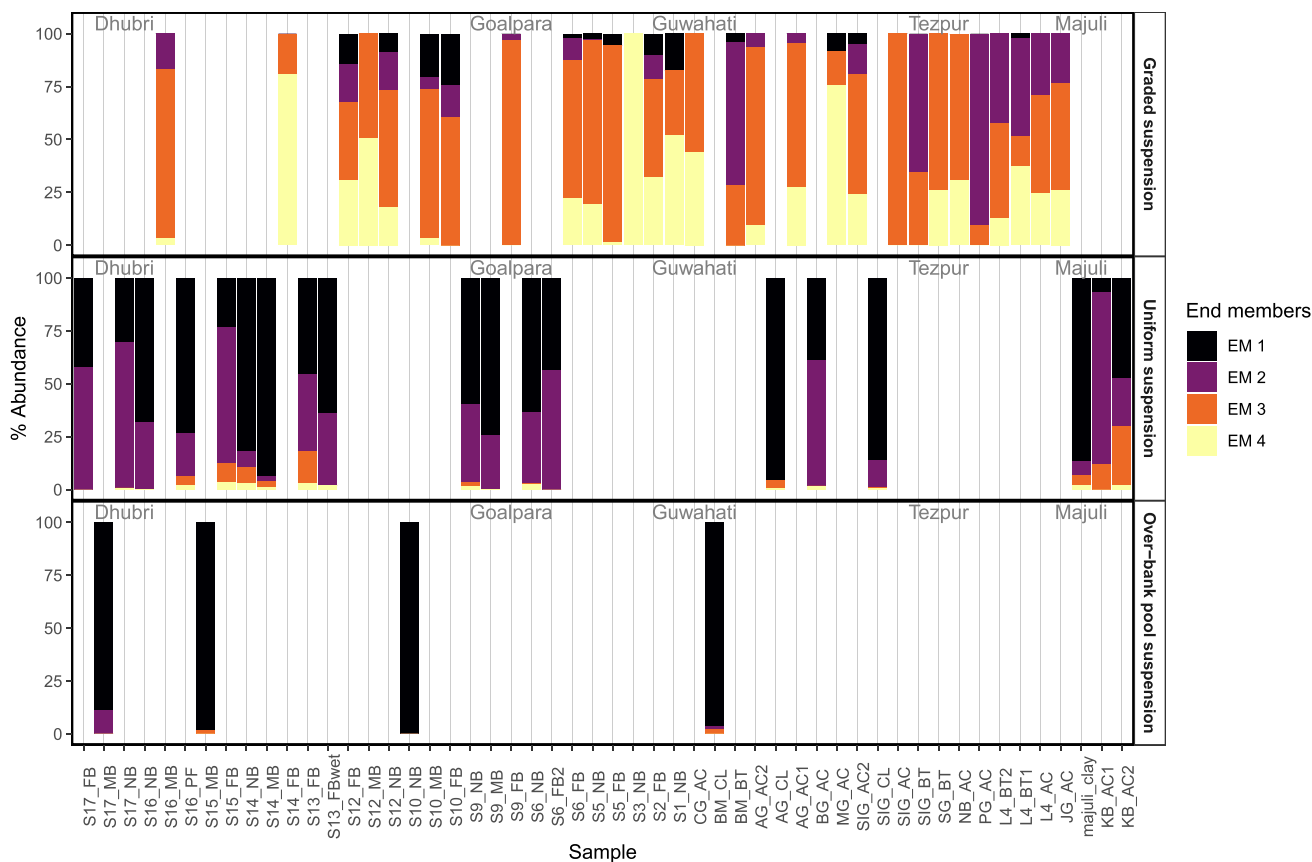
Fig. 6 End-member abundances at different locations along the main trunk of the Brahmaputra River corresponding to the deposition environment of C-M plot (Fig. 4)

Table 2 Average abundance (%) of grain-size end-members in three deposition environment

	EM 1	EM 2	EM 3	EM 4
Over-bank pool suspension	96.0	3.15	0.84	0.00
Graded suspension	4.35	16.8	52.9	25.9
Uniform suspension	61.5	34.2	2.81	1.47

up to Dhubri does not show any increase in this size range in downstream sections. Similarly, the study by Singh et al. (2007) in the Ganga floodplains did not reveal any systematic increase in this size range. However, their data showed a sharp increase in the proportions of the 63–125 μm size range near the delta, with proportions ranging from approximately 10–20% in the floodplains to approximately 50% in the delta.

Fig. 7 XRD scans of the 54 samples analyzed in this study, illustrating the mineral composition. Smt: smectite, SS: sheet silicates, Amb: amphibole, Chl: chlorite, Q: quartz, F: feldspar. The inset displays a crossplot of the intensity ratio of quartz to sheet silicates against the median grain size. The shaded portion represents the grain-size range of 63–172 μm, which contains a relatively smaller number of samples
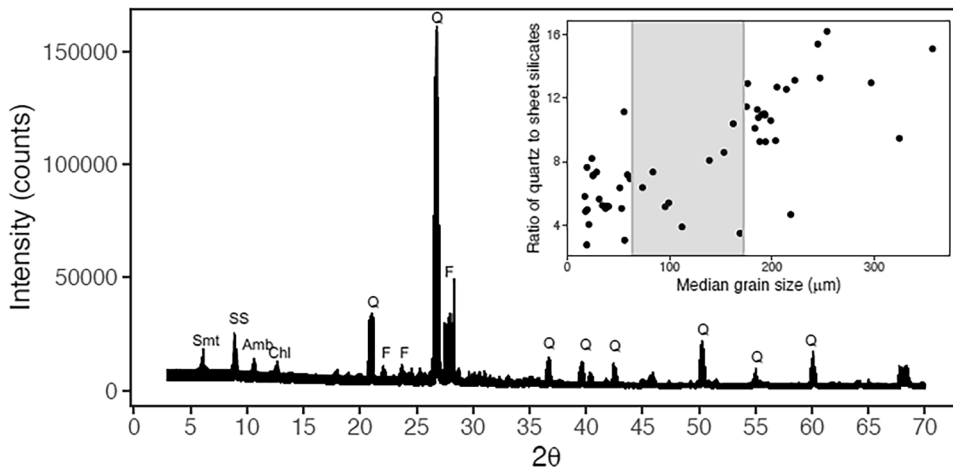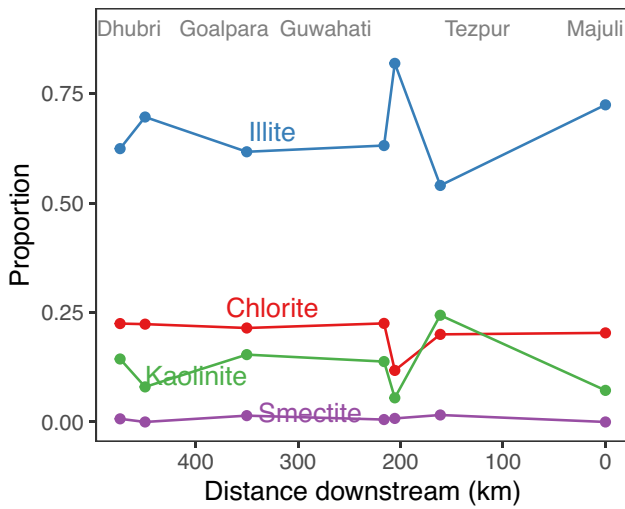
Fig. 8 Downstream variation of clay mineral proportion in the main trunk of the Brahmaputra

The deposition of too-fine (ca. 20 μm) sediments floodplain sandbars can be attributed to favorable conditions for deposition, such as low-flow zones over bar slopes (Fig. 3b) and bar depressions (Fig. 3f), during periods of slow recession when there is sufficient time for fine-grained sediments to settle (Fig. 3d and e). Notably, too-fine sediments are consistently present in uniform suspension in the water column regardless of the discharge conditions. Therefore, the deposition of too-fine sediments is primarily controlled by favorable deposition conditions rather than flow conditions. However, these favorable conditions are more likely to occur during receding or low flood periods.

In summary, the presence of too-coarse sediments in the floodplains can be attributed to hydraulic sorting during peak flood events, leading to the selective transport and depletion of fine-grained sediments. The intermediate size range of 63–172 μm tends to travel further downstream in graded suspension, in accordance with the burst-sweep mechanism as proposed by Singh et al. (2007), which explains the bedload sediment transport in graded suspension through bursts and sideways deposition sweeps. Coarse-grained sediments would also enter graded suspension but travel shorter distances due to their larger size. Over time, repeated annual floods result in a coarsening of the riverbed, with deposition of the 63–172 μm size range occurring predominantly in downstream regions such as deltas, where favorable conditions for deposition may exist. The transport and deposition of too-fine sediments (20 μm) differ from other sediment sizes. These sediments are consistently transported in uniform suspension, spanning nearly two-thirds of the upper water column. Due to their perennial availability, they have the potential to be deposited within floodplains under favorable conditions, such as the presence of low-flow zones over bar tops, slopes, or depressions.

5.3 Downstream variability of grain-size distribution

We interpret the downstream grain-size variation with the river's morphological conditions. The river width and river braiding index measured during the non-monsoon period is taken from Sarma and Acharjee (2018). The downstream variation in grain size is influenced by nodal points along the river, particularly at Tezpur and Guwahati. Among these, Guwahati stands out as the most prominent nodal point, coinciding with the narrowest width and low braiding index within the floodplains (Fig. 10). At these nodal points, the stream power increases creating conducive conditions to net sediment transport, leading to an increase in grain size as finer material is more easily transported.

Fig. 9 Depth profiles of suspended sediment concentration and median grain size (d50 μm) in Ganga and Brahmaputra River in Bengal Delta before their confluence (Fig. 1a). Data for Ganga and Brahmaputra profiles are taken from Lupker et al. (2011) and Garzanti et al. (2011). The horizontal boxplot represents the median grain sizes of samples characterized in two deposition environments as shown in Fig. 4
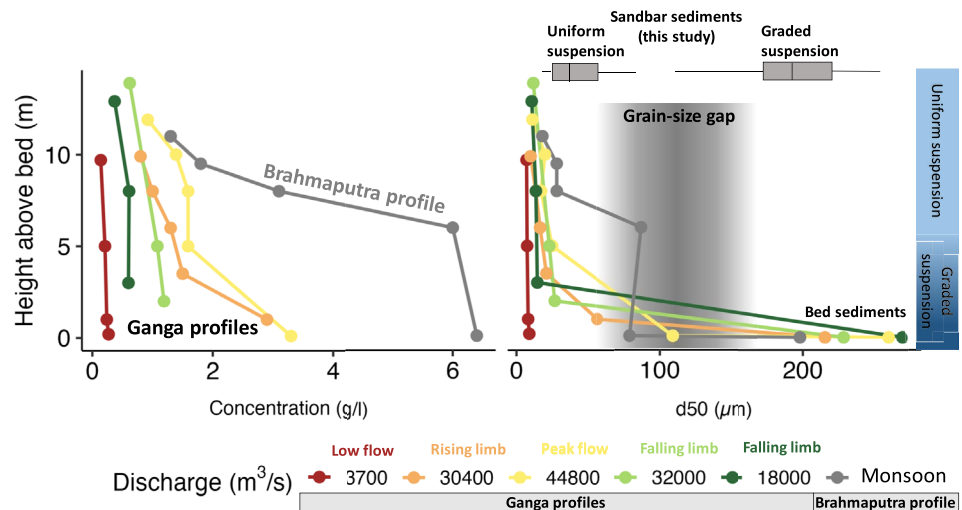
Goswami (1985) estimated that the reach partially including the Guwahati nodal point experienced net degradation of 2.55 cm (Fig. 10), while the upstream and downstream reaches of Guwahati exhibited net channel aggradation. Our data aligns with this characteristic behavior of the river. As the river width decreases approaching Guwahati, there is an increase in the median grain size, and the sediments are dominated by the coarse end-members (EM 1, EM 2). Similarly, near Tezpur, there is a higher abundance of the coarse end-members. As the river reaches downstream, where it widens into multiple channels (Fig. 1), there is a higher occurrence of fine-grained sediments.

It is important to note that our inference regarding nodal points controlling sediment grain-size distribution remains partially unconstrained due to the limited number of data points in our study. While we have established the influence of local variations on grain-size distributions within a single location, it is crucial to recognize

that individual samples, particularly those obtained after the Guwahati nodal point, may not represent the average sediment grain-size distribution of such a wide channel (ca. 15 km). Therefore, further research employing a finer spatial resolution sampling strategy could reveal intriguing patterns of grain-size distribution and provide a more comprehensive understanding of nodal point effects.

5.4 Implications for grain-size gap studies

The grain-size gap in sediment deposits exists in other fluvial environments. For instance, gravel-bed rivers typically exhibit a bimodal distribution with a grain-size gap typically ranging from 1000 to 5000 μm (Lamb and Venditti 2016). The absence of material in this range can be attributed to two possible explanations, as discussed by Dingle et al. (2021). Firstly, selective transport of the grain-size gap sediments is supported by the
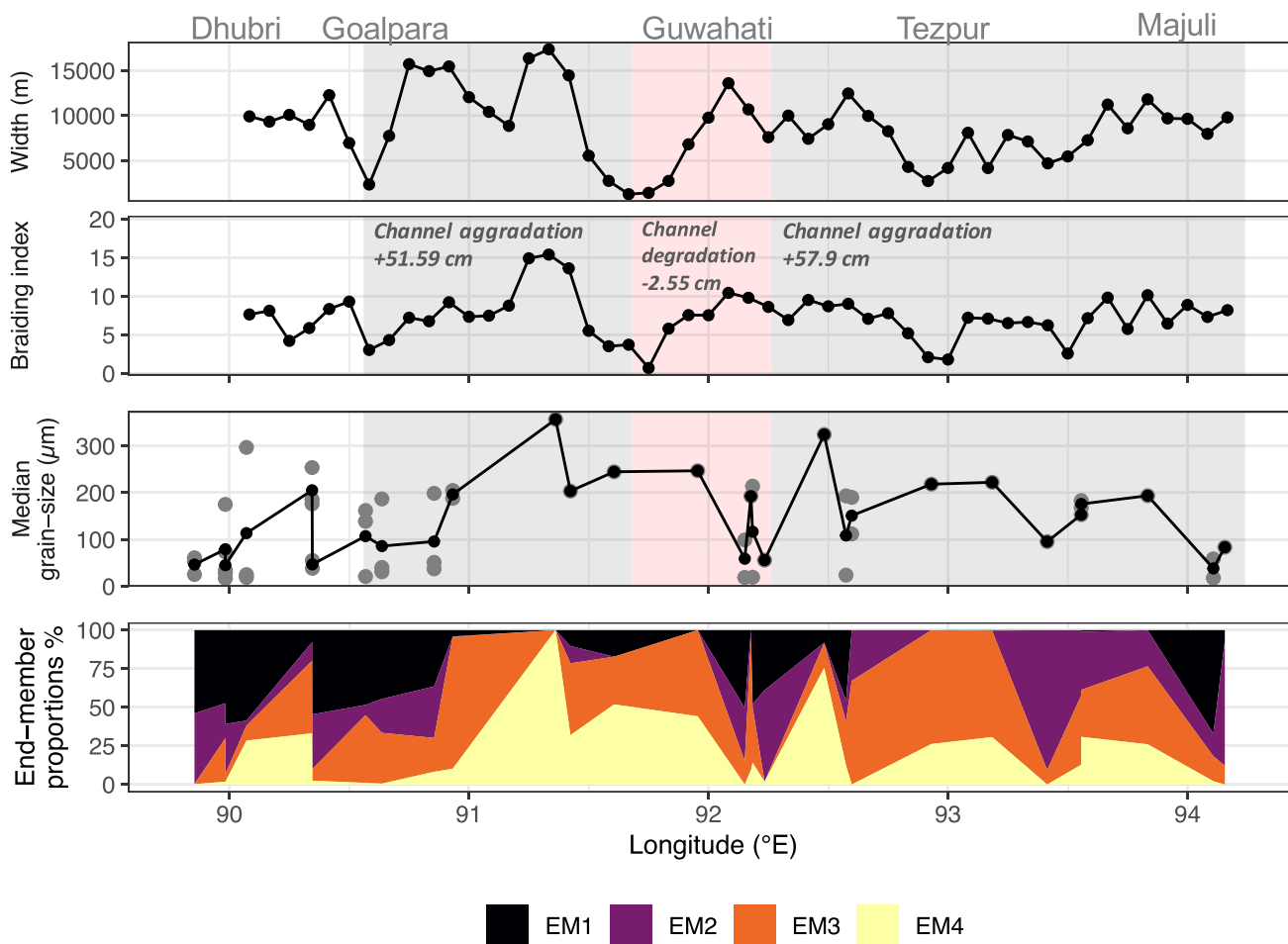

Fig. 10 Variation of river width and braiding index of the Brahmaputra main trunk. Data is taken from (Sarma and Acharjee 2018). The mean of the median grain size of each location are shown in dark solid line and dots, while the median of each sample at that location are shown with gray dots. The zones and values of aggradation (shaded gray) and degradation (shaded red) are taken from Goswami (1985). End-member abundances are shown by area plot

superior mobility of these sediments, which is attributed to the influx of finer sediments, leading to filling and smoothening of the bed surface and increased fluid acceleration near the bed surface (Venditti et al. 2010). Secondly, the absence of this material could be due to the separation of transport modes for gravel and sand. As shown by Lamb and Venditti (2016), the lack of this material may result from a river's inability to transport sand as wash load when bed shear velocities drop below approximately 0.1 m s^{-1}, causing the material within the grain-size gap to fall only within the fine tail or coarse tail of sediment deposits.

In our study, we find evidence of the grain-size gap occurring between the modes of silt and sand (Fig. 11a) in the sand-bed floodplains. This grain-size gap primarily appears as an inter-sample phenomenon, indicating selective transport of material <172 μm from the bed through repeated fluvial processes, and the preferential deposition of material <63 μm during favorable

low-flow conditions. These processes essentially lead to the formation of the grain-size gap between these two-grain sizes.

Interestingly, although not widely reported and discussed, grain-size gaps between samples also exist in other sand-bed rivers. For instance, as previously discussed, grain-size data of Singh et al. (2007) show that Ganga floodplain sediments primarily fall into two size ranges: 125–250 μm and <63 μm, with a paucity of samples in the size range of 63–125 μm. Similarly, Wang et al. (2009) data from the Yangtze River in China show that the majority of samples lie in sizes >200 μm and <100 μm, with a scarcity of samples in the 100–200 μm range. Additionally, Szmańda (2018) reported a grain-size gap in the size range of 125–250 μm in over-bank deposits of Polish rivers, and Ta et al. (2011) identified a paucity of samples in the size range of 80–100 μm in the Yellow River, China; however, they attributed this scarcity to the effect of upstream dams.
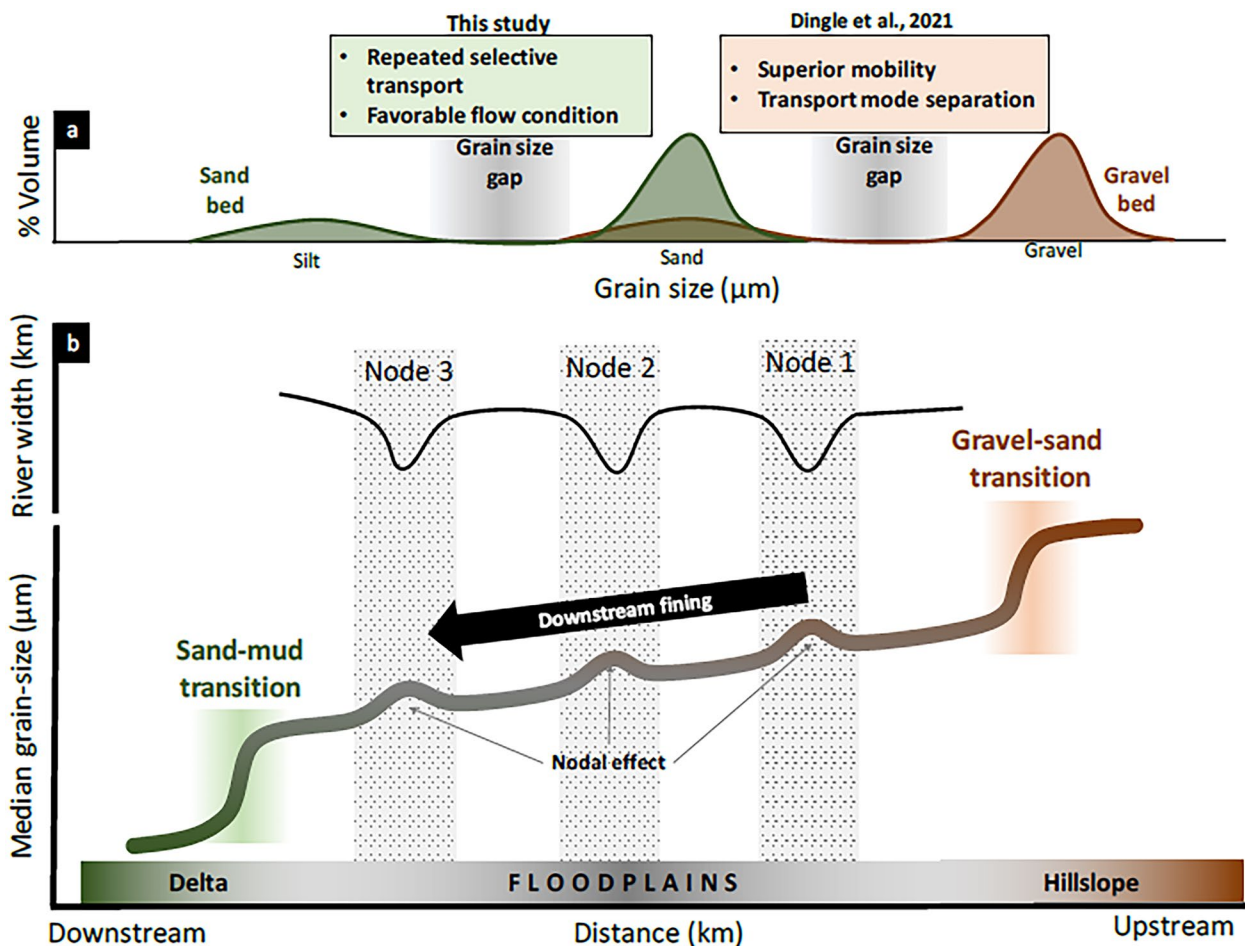

Fig. 11 Schematic illustrating **a** the grain-size gap observed in gravel-bed rivers and sand-bed rivers, along with their possible causes as reported previously and by this study, respectively, and **b** the disrup-tion of downstream fining by river nodes, as well as the occurrences of gravel-sand and sand-mud transitions near hillslope and delta zones, respectively

5.5 Implications for downstream fining studies

Our hypothesis regarding the repeated flushing out of grain-size gap material from the floodplains finds support in the deposits observed near the river mouth of other rivers (e.g., Singh et al. 2007; Wang et al. 2009; Luo et al. 2012; Kästner et al. 2017; Morón and Amos 2018). Near the river mouth, there is a notable increase in the proportion of sediments within a size range that is less dominant in the floodplains. For example, the Ganga estuary shows a sharp increase (approximately from 20% to 50%) in the proportion of 63–125 μm sized sediments, which was less dominant in the floodplain (Singh et al. 2007). Similarly, the Yangtze River's anabranching system also demonstrated a sharp change in grain size below 200 μm (Wang et al. 2009; Luo et al. 2012). The deposition of fine sediments near river mouths can be attributed to favorable conditions for deposition (Morón and Amos 2018), influenced by tidal effects (Luo et al. 2012; Kästner et al. 2017), as the river transitions from fluvial to tidal zones. Thus, these zones exhibit a distinct pattern of an abrupt decrease in the median grain size, akin to the transition seen in hillslope-floodplain transition zones (e.g., Constantine et al. 2003; Singh et al. 2007; Singer 2008; Dingle et al. 2021) as illustrated in Fig. 11b.

Overall, sand-bed rivers display a downstream fining trend, which can be locally disrupted by lateral tributaries joining the main channel, resulting in local maxima in the downstream fining trend (e.g., Singh et al. 2007; Ta et al. 2011; Luo et al. 2012; Pan et al. 2015). In the case of the Brahmaputra, a similar effect is likely to occur due to river nodes characterized by narrower river widths and low braiding indices. These conditions would increase stream power (Wang et al. 2009)

and facilitate net sediment transport from these narrow zones, with fine sediments preferentially flushing out and increasing the median grain size. The effect of lateral tributaries in the Brahmaputra River may not be significant, as the floodplain sediments are dominated by sediments from a single source, the Eastern Syntaxis in the Siang Valley. Approximately 60% of the sediment at Guwahati and 30–45% of the sediment at Dhubri originates from the Siang Valley, while the remaining ca. 50% of sediments come from all other northern and southern tributaries (Singh and France-Lanord 2002; Garzanti et al. 2004; Singh 2006; Lupker et al. 2017). Additionally, our data shows that while sediment upstream of the Siang (at Yingkiong, Fig. 1b) is quite coarse, by the time it reaches Pasighat, the grain-size distribution has attained similar characteristics to the floodplain sediments (Fig. 2).

5.6 Downstream variability of mineral composition in floodplains

The mineral composition of sediment in the floodplain can be influenced by both lithological sources from different tributaries and various physical and chemical processes. However, in the case of the Brahmaputra floodplains, the role of lithology in changing sediment composition can be disregarded as the primary factor for two reasons. Firstly, the sediment in the Brahmaputra is predominantly derived from a single sediment source, namely Eastern Syntaxis (Fig. 1). Secondly, even if there were sediment sources from multiple tributaries, the floodplains tend to homogenize the lithological signature (Ramesh et al. 2000). Therefore, variations in floodplain sediment composition are primarily attributed to physical and chemical processes.

Fig. 12 Downstream variation of quartz to feldspar ratio, with dot-size representing median grain size of samples
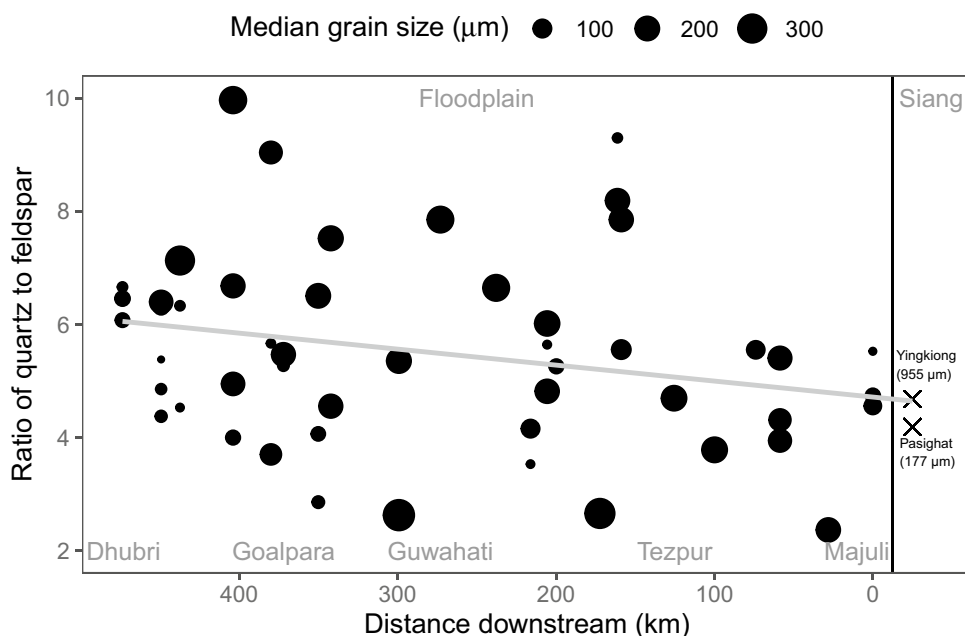
To investigate the weathering patterns in the floodplains, we utilized the intensity ratios of XRD peaks of quartz and feldspar as a proxy for chemical weathering. We observed quartz to feldspar ratio varying from ca. 2 to 8 with a mean of 5. This range is approximately close to the quartz to feldspar ratio observed through the petrographic data (range: 2–5, mean: 3) by Garzanti et al. (2004, 2010) in the floodplains sediments. Based on our data, we observed slightly higher quartz to feldspar ratio in the downstream reach from Goalpara to Dhubri (Fig. 12), where the river width and braiding index are higher (Fig. 10), and the river is bifurcating into several channels (Fig. 1. Previous petrographic analyses of Brahmaputra floodplain sediments have indicated that the sediments undergo limited weathering, primarily related to the weathering of carbonates (Garzanti et al. 2004). Our clay mineralogy data also does not reveal any significant changes in the clay assemblage, with kaolinite proportions remaining consistent (Fig. 8), indicating that the weathering is low, and is limited to easily weathered grains such as carbonates, olivine and pyroxene. The low intensity of weathering is attributed to the rapid transfer of sediments in the Brahmaputra floodplains (Singh and France-Lanord 2002). The slightly higher chemical weathering signal in the lower reaches of the Brahmaputra near Dhubri may be attributed to the longer residence time of sediments in that area. Additionally, the lower reaches receive higher rainfall compared to the upper parts (Sarma 2004), which can also contribute to increased weathering effects.

6 Conclusion

In this study, we applied bulk mineralogy, clay mineralogy, and end-member modeling on grain size to investigate sediment characteristics and variations in the Brahmaputra River floodplains. Mineralogical composition in the floodplains remains largely the same with, a minor increase in quartz to feldspar ratio downstream. Additionally, our findings shed light on sediment transport and deposition processes in river floodplains, particularly with implications for downstream fining and the existence of a grain-size gap. The grain-size distribution of sandbars within the floodplain exhibits variability, with median grain sizes mostly centered near 20 μm and 200 μm. Local flow conditions, such as over-bank pool suspension, influence the grain-size distribution at specific locations. Sandbar deposits, however, are primarily formed by the sediment transported in uniform and graded suspension.

We observed a limited number of samples in sandbar deposits falling within the size range of approximately 63–172 μm, which is consistent with the grain-size gap commonly found in sand-bed rivers worldwide but has remained under-discussed. Utilizing the existing depth profile sediment grain-size data, we propose that the selective transport of sediments within this grain-size gap occur during repeated annual peak floods, leading to the coarsening of the riverbed, with a median size of approximately 200 μm. Meanwhile, the fine sediments (20 μm) are perennially transported in uniform suspension and can be deposited within floodplains under favorable low-flow conditions. The proposed transport mechanism gains support from the presence of accumulated sediments within the grain-size gap range near the river mouth, as observed in other sand-bed rivers. This results in a distinct sand-mud transition zone, characterized by a sharp decrease in grain size.

Moreover, the downstream variation in grain-size distribution is influenced by the presence of bedrock confined zones or "nodes'' along the river. These nodes, characterized by narrower widths and lower braiding index, exhibit an increase in grain size, similar to the effect of tributary confluence in the main channel, which also increases the grain size. However, further sampling at a finer spatial resolution is necessary to strengthen our observations of this pattern.

Data Availability The datasets used in this study are available from the corresponding author upon reasonable request.

Declarations

Conflict of interest The authors declare no competing interests.

References

Biscay PE (1965) Mineralogy and sedimentation of recent deep-sea clay in the Atlantic Ocean and adjacent seas and oceans. Geol Soc Am Bull 76(7):803–832

Bouchez J, Gaillardet J, Lupker M, Louvat P, France-Lanord C, Maurice L, Armijos E, Moquet JS (2012) Floodplains of large rivers: weathering reactors or simple silos? Chem Geol 332:166–184

Constantine CR, Mount JF, Florsheim JL (2003) The effects of longitudinal differences in gravel mobility on the downstream fining pattern in the Cosumnes River. California. J Geol 111(2):233–241

Dingle EH, Kusack KM, Venditti JG (2021) The gravel-sand transition and grain size gap in river bed sediments. Earth Sci Rev 222:103838

Dixit A, von Eynatten H, Schönig J, Karius V, Mahanta C, Dutta S (2023) Intra-seasonal variability in sediment provenance and transport processes in the Brahmaputra basin. J Geophys Res: Earth Surf 128(6):e2023JF007105

Frings RM (2008) Downstream fining in large sand-bed rivers. Earth Sci Rev 87(1–2):39–60

Galy A, France-Lanord C (2001) Higher erosion rates in the Himalaya: geochemical constraints on riverine fluxes. Geology 29(1):23–26

Garzanti E (2019) The Himalayan Foreland Basin from collision onset to the present: a sedimentary-petrology perspective. Geol Soc, Lond, Special Publications 483(1):65–122

Garzanti E, Andó S, France-Lanord C, Censi P, Vignola P, Galy V, Lupker M (2011) Mineralogical and chemical variability of fluvial sediments. 2. Suspended-load silt (Ganga-Brahmaputra, Bangladesh). Earth Planet Sci Lett 302(1–2):107–120

Garzanti E, Andò S, France-Lanord C, Vezzoli G, Censi P, Galy V, Najman Y (2010) Mineralogical and chemical variability of fluvial sediments. 1. Bedload sand (Ganga-Brahmaputra, Bangladesh). Earth Planet Sci Lett 299(3–4):368–381

Garzanti E, Vezzoli G, Andò S, France-Lanord C, Singh SK, Foster G (2004) Sand petrology and focused erosion in collision orogens: the Brahmaputra case. Earth Planet Sci Lett 220(1–2):157–174

Gemignani L, van der Beek P, Braun J, Najman Y, Bernet M, Garzanti E, Wijbrans J (2018) Downstream evolution of the thermochronologic age signal in the Brahmaputra catchment (eastern Himalaya): implications for the detrital record of erosion. Earth Planet Sci Lett 499:48–61

Goswami DC (1985) Brahmaputra river, Assam, India: physiography, basin denudation, and channel aggradation. Water Resour Res 21(7):959–978

He Z, Sun Z, Li Y, Zhao Q, Hu Y, Chen Z (2022) Response of the gravel-sand transition in the Yangtze River to hydrological and sediment regime changes after upstream damming. Earth Surf Process Landf 47(2):383–398

He Z, Sun Z, Zhou W, Li Y, Hu Y (2023) Gravel-sand transition of the Yangtze river: human disturbances, migration processes, and controlling factors. J Geophys Res: Earth Surf 128(6): e2022JF006984

Islam MR, Begum SF, Yamaguchi Y, Ogawa K (1999) The Ganges and Brahmaputra rivers in Bangladesh: basin denudation and sedimentation. Hydrol Process 13(17):2907–2923

Johnsson MJ (1993) The system controlling the composition of clastic sediments. In Processes Controlling the Composition of Clastic Sediments, pages 1–20. Geol Soc of Am Special Pap

Kästner K, Hoitink A, Vermeulen B, Geertsema T, Ningsih N (2017) Distributary channels in the fluvial to tidal transition zone. J Geophys Res: Earth Surf 122(3):696–710

Khan MHR, Liu J, Liu S, Seddique AA, Cao L, Rahman A (2019) Clay mineral compositions in surface sediments of the Ganges-Brahmaputra-Meghna river system of Bengal Basin, Bangladesh. Marine Geol 412:27–36

Lamb MP, Venditti JG (2016) The grain size gap and abrupt gravel-sand transitions in rivers due to suspension fallout. Geophys Res Lett 43(8):3777–3785

Ludwikowska-Kędzia M (2013) The assemblages of transparent heavy minerals in Quaternary sediments of the Kielce-Łagów Valley (Holy Cross Mountains, Poland). Geologos 19(1–2):95–129

Luo X, Yang S, Zhang J (2012) The impact of the Three Gorges Dam on the downstream distribution and texture of sediments along the middle and lower Yangtze River (Changjiang) and its estuary, and subsequent sediment dispersal in the East China Sea. Geomorphology 179:126–140

Lupker M, France-Lanord C, Galy V, Lavé J, Gaillardet J, Gajurel AP, Guilmette C, Rahman M, Singh SK, Sinha R (2012) Predominant floodplain over mountain weathering of Himalayan sediments (Ganga basin). Geochimica et Cosmochimica Acta 84:410–432

Lupker M, France-Lanord C, Lavé J, Bouchez J, Galy V, Métivier F, Gaillardet J, Lartiges B, Mugnier JL (2011) A Rouse-based method to integrate the chemical composition of river sediments: application to the Ganga basin. J Geophys Res 116(F4)

Lupker M, Lavé J, France-Lanord C, Christl M, Bourlès D, Carcaillet J, Maden C, Wieler R, Rahman M, Bezbaruah D, Xiaohan L (2017) 10 Be systematics in the Tsangpo-Brahmaputra catchment: the cosmogenic nuclide legacy of the eastern Himalayan syntaxis. Earth Surf Dyn 5(3):429–449

Milliman JD, Farnsworth KL (2011) River discharge to the coastal ocean. Cambridge University Press, Cambridge

Morón S, Amos KJ (2018) Downstream grain-size changes associated with a transition from single channel to anabranching. Sedimentology 65(5):1590–1610

Musselman ZA, Tarbox AM (2013) Downstream trends in grain size, angularity, and sorting of channel-bed and bank deposits in a coastal plain sand-bed river: the Pascagoula River system, Mississippi, USA. Southeastern Geographer 53(2):177–197

Nandi KK, Pradhan C, Dutta S, Khatua KK (2022) How dynamic is the Brahmaputra? Understanding the process-form-vegetation interactions for hierarchies of energy dissipation. Ecohydrology 15(3):e2416

Pan B, Pang H, Zhang D, Guan Q, Wang L, Li F, Guan W, Cai A, Sun X (2015) Sediment grain-size characteristics and its source implication in the Ningxia-Inner Mongolia sections on the upper reaches of the Yellow River. Geomorphology 246:255–262

Passega R (1964) Grain size representation by cm patterns as a geologic tool. J Sediment Res 34(4):830–847

Passega R, Byramjee R (1969) Grain-size image of clastic deposits. Sedimentology 13(3–4):233–252

Paterson GA, Heslop D (2015) New methods for unmixing sediment grain size data. Geochemistry, Geophys, Geosystems 16(12):4494–4506

Prins MA, Weltje GJ (1999) End-member modeling of siliciclastic grain-size distributions: the late Quaternary record of Eolian and fluvial sediment supply to the Arabian Sea and its paleoclimatic significance. In Numerical Experiments in Stratigraphy: Recent Advances in Stratigraphic and Sedimentologic Computer Simulations. SEPM Society for Sedimentary Geology

Ramesh R, Ramanathan P, Ramesh S, Purvaja R, Subramanian V (2000) Distribution of rare earth elements and heavy metals in the surficial sediments of the Himalayan river system. Geochemical J 34(4):295–319

Rice SP, Church M (2010) Grain-size sorting within river bars in relation to downstream fining along a wandering channel. Sedimentology 57(1):232–251

Sarma J (2004) An overview of the Brahmaputra river system. The Brahmaputra basin water resources. Springer, Netherlands, Dordrecht, pp 72–87

Sarma J (2005) Fluvial process and morphology of the Brahmaputra River in Assam. India. Geomorphology 70(3–4):226–256

Sarma JN, Acharjee S (2018) A study on variation in channel width and braiding intensity of the Brahmaputra River in Assam. India. Geosciences 8(9):343

Singer MB (2008) Downstream patterns of bed material grain size in a large, lowland alluvial river subject to low sediment supply. Water Resour Res 44(12)

Singh M, Singh IB, Müller G (2007) Sediment characteristics and transportation dynamics of the Ganga River. Geomorphology 86(1–2):144–175

Singh SK (2006) Spatial variability in erosion in the Brahmaputra basin: causes and impacts. Curr Sci 90(10):1272–1275

Singh SK, France-Lanord C (2002) Tracing the distribution of erosion in the Brahmaputra watershed from isotopic compositions of stream sediments. Earth Planet Sci Lett 202(3–4):645–662

Szmańda J (2018) Main determinants of the grain size distribution of overbank deposits in Poland-an overview of literature on models of sedimentation. Geol Q 62(4):873–880

Ta W, Wang H, Jia X (2011) Downstream fining in contrasting reaches of the sand-bedded Yellow River. Hydrol Process 25(24):3693–3700

Van Hateren J, Prins M, Van Balen R (2018) On the genetically meaningful decomposition of grain-size distributions: a

comparison of different end-member modelling algorithms. Sediment Geol 375:49–71

Venditti J, Dietrich W, Nelson P, Wydzga M, Fadde J, Sklar L (2010) Mobilization of coarse surface layers in gravel-bedded rivers by finer gravel bed load. Water Resour Res 46(7)

von Eynatten H, Tolosana-Delgado R, Karius V (2012) Sediment generation in modern glacial settings: grain-size and source-rock control on sediment composition. Sediment Geol 280:80–92

von Eynatten H, Tolosana-Delgado R, Karius V, Bachmann K, Caracciolo L (2016) Sediment generation in humid Mediterranean setting: grain-size and source-rock control on sediment geochemistry and mineralogy (Sila Massif, Calabria). Sediment Geol 336:68–80

Wang Z, Chen Z, Li M, Chen J, Zhao Y (2009) Variations in downstream grain-sizes to interpret sediment transport in the middle-lower Yangtze River, China: a pre-study of Three-Gorges Dam. Geomorphology 113(3–4):217–229

Wasson R, Acharjee S, Rakshit R (2022) Towards identification of sediment sources, and processes of sediment production, in the Yarlung-Tsangpo-Brahmaputra River catchment for reduction of fluvial sediment loads. Earth Sci Rev 226:103932

Weltje GJ (1997) End-member modeling of compositional data: numerical-statistical algorithms for solving the explicit mixing problem. Math Geol 29(4):503–549

Weltje GJ, von Eynatten H (2004) Quantitative provenance analysis of sediments: review and outlook. Sediment Geol 171(1–4):1–11